Joint Active Beamforming and Circuit Parameter Optimization for Reconfigurable Intelligent Surface-aided SWIPT Systems

Ruoyan Ma*, Jie Tang*, Xiuyin Zhang*, Kai-Kit Wong†, and Jonathon A. Chambers ‡
*School of Electronic and Information Engineering, South China University of Technology, Guangzhou, China
† Department of Electronic and Electrical Engineering, University College London, WClE 6BT London, U.K.
‡School of Engineering, University of Leicester, Leicester LE1 7RH, U.K.
Email: eeruoyan_ma@mail.scut.edu.cn

***Abstract*—The simultaneous wireless information and power transfer (SWIPT) technology assisted by the reconfigurable intelligent surface (RIS) can bring flexibility and stability to the end nodes of the internet of things (IoT) during the deployment. In this paper, we propose a RIS-aided SWIPT system based on a hardware transfer model from the electromagnetic perspective. Particularly, an energy efficiency (EE) maximization problem subject to the quality of service (QoS) demands, power resource budget and circuit restrains is introduced. Furthermore, the active beamforming vectors of the BS and the circuit parameters at the RIS are optimized jointly. The problem can be decomposed into two sub-problems and solved iteratively until convergence. In particular, semi-definite relaxation (SDR), successive convex approximation (SCA), Dinkelbach's algorithm are applied to the solutions of the sub-problems. Numerical results reveal the influences of the various QoS requirements on EE performance. Moreover, the actual generated beams of the BS and the RIS are shown to demonstrate the effectiveness of the proposed optimization strategy.**

***Index Terms*—Electromagnetism, RIS, SWIPT, energy efficiency.**

I. Introduction

For bearing more terminal devices, the power consumption will climb significantly in the sixth generation (6G) wireless communication [1]. As for the key application scenario of 6G, the internet of things (IoT), this situation is more prominent owing to its large-scale distribution and countless nodes [2], [3]. Many approaches are proposed to reduce the energy dissipation of nodes as much as possible, e.g., by introducing the range-based location system to remove high-power-consumption positioning devices and algorithms [4]. Moreover, in order to further facilitate practical deployment of the IoT and realize the goal of green communication, simultaneous wireless information and power transfer (SWIPT) technology can be introduced to meet nodes' requirements of information exchange and power supply at the same time [5]. In the general sense, SWIPT is arranged at the far-filed condition for achieving greater system flexibility. Its critical hardware device is the rectenna, which consists of the receiving antenna and the rectifying circuit. They are responsible for catching electromagnetic (EM) power and outputting DC power, respectively [6].

However, to guarantee the quality of service (QoS), SWIPT has strict requirements on the transmission links. Particularly, the transfer may be interrupted easily, when line-of-sight (LoS) links are obstructed. Thanks to the reconfigurable intelligent surface (RIS), the links can be reconstructed and the stability of the system is enhanced [7], [8]. The idea of RIS can be traced back to the reconfigurable two-dimension metasurface [9]. As having the ability to control the channel environment with its reflecting attribute, it is known as the promising technology in 6G [2]. Generally, A RIS has control circuits, a reflecting backplane and an element array [7]. After sensing the environmental information, the RIS can operate the control circuits to adjust the statuses of the elements for adjusting the transfer links according to the demands of the scenario deployments.

As a kind of electromagnetic equipment, the reflection characteristics of the RIS rely on multiple factors, e.g., types of reflection elements, control approaches, and array configurations. Hence the modeling of it should be full-scale and down-to-earth. Considering the simplicity of the modeling, the independent diffusive scatterer (IDS) RIS model is the best choice. However, this model may be too simple to expose the crucial features of the RIS [10]. Unlike it, the physics model [11] based on the radar theory and impedance model [12] extracted from the equivalent-circuit analysis are proposed to show the hardware characteristics of the RIS. Besides, the transfer model based on electromagnetism is also proposed to bring a new perspective to system analysis [13]. On account of that different models descript the RIS from diverse views, the optimizable variables of them may also be distinct. In particular, some are performance indicators (i.e., reflection coefficients [14]), while some are hardware parameters (i.e., circuit impedances [13]).

In our work, after weighing solvability and accuracy of the modeling, we utilize the EM end-to-end transfer model [13] to construct the RIS-aided SWIPT system. The optimizable variables of the RIS are practical impedance parameters of the control circuits. Thanks to it, the hardware characteristics of the RIS are taken into consideration. Concretely, the problem can be decomposed into two sub-problems with the alternative

strategy. Both of them are transformed by the semi-definite relaxation (SDR) method and then the optimization framework based on the successive convex approximation (SCA) and Dinkelbach's algorithm is introduced to tackle them.

II. System Model

We consider a MISO downlink RIS-aided SWIPT system with separated information and energy receivers. From the actual deployment, the energy receivers (ERs) should be closer to the base station (BS) than the information receivers (IRs) owing to that ERs are more sensitive to the received power. Moreover, since IRs are easier to be blocked at longer transmission distances, the BS-IR links are assumed to be nonexistent in our work. The element numbers of the BS and the RIS are N_t and N_i. All transmission ends in this paper are set on the same 2-dimension plane.

For the transfer model, we assume that all antennas of BS, IRs, ERs and RIS are dipole antennas, which coincides with the setting in [13]. With this assumption, we can introduce the EM transfer model proposed in [13] to construct the total link, which is assisted by the RIS, between BS and receivers as following

$$\mathbf{h}_e = \mathbf{d} + \mathbf{c}\left(\mathbf{Z}_{ii} + \mathbf{\Xi}\right)^{-1}\mathbf{K}. \tag{1}$$

where $\mathbf{Z}_{ii}$ and $\mathbf{\Xi}$ represent the self-impedance matrix of the RIS and the impedance matrix of the control board. In addition, other parameters can be calculated as

$$\frac{\mathrm{Z}_l}{\mathrm{Z}_l + \mathrm{Z}_{rr}}\mathbf{Z}_{rt}\left(\mathbf{Z}_g + \mathbf{Z}_{tt}\right)^{-1} = \mathbf{d}, \tag{2}$$

$$-\frac{\mathrm{Z}_l}{\mathrm{Z}_l + \mathrm{Z}_{rr}}\mathbf{Z}_{ri} = \mathbf{c}, \tag{3}$$

$$\mathbf{Z}_{it}\left(\mathbf{Z}_g + \mathbf{Z}_{tt}\right)^{-1} = \mathbf{K}, \tag{4}$$

$\mathbf{Z}_g$ and Z_l are the source impedance matrix and the load impedance. $\mathbf{Z}_{xy}$ in the above equations denote the mutual-impedance matrices between different ends or the self-impedance matrices of them. Moreover, the entries of the matrices can be calculated according to Lemma 2 in [13].

Except for the deterministic EM links, other multipath links based on the randomly occurring scatterers are also considered in our work. Particularly, the scatterer links are shown as

$$\mathbf{h}_c = \sqrt{\frac{N_i}{N_{\mathrm{path,total}}}}\sum_{p=1}^{N_{\mathrm{sca}}}\sum_{q=1}^{N_{\mathrm{path},p}}\beta_{p,q}\sqrt{PL\left(r_{p,q}\right)}\mathbf{a}_t\left(\phi_{p,q}^t\right), \tag{5}$$

The above equation has the same form in [15] and it describes the sum of the random links. N_{sca} and N_{path} represent the numbers of the scatterer clusters and the paths in each cluster. $N_{\mathrm{path,total}}$ denotes the sum of the paths. $\beta_{p,q}$, $PL\left(r_{p,q}\right)$ and $\mathbf{a}_t$ are the complex gain, path loss and transmitting array response vector. In particular, $\mathbf{a}_t(\phi_{p,q}^t) = \frac{1}{\sqrt{N_t}}\left[1, \ldots, e^{j(N_t-1)k_0 d_0 \sin(\phi_{p,q}^t)}\right]$ and $r_{p,q} = r_p + \sqrt{\left(r_p \sin\theta_{p,q}^t\right)^2 + \left(d - r_p\cos\theta_{p,q}^t\cos\phi_{p,q}^t\right)^2}$, where r_p is the distance between BS and clusters. d is the distance between BS and receivers. $\theta_{p,q}^t$, and $\phi_{p,q}^t$ are the angles of departure.

The total links including the EM links and scatterer links can be presented as

$$\tilde{\mathbf{h}} = \mathbf{h}_e + \mathbf{h}_c. \tag{6}$$

We consider both the energy beamforming and the information beamforming. Then the received signal model of the m_{th} receiver can be shown as

$$y_m = \tilde{\mathbf{h}}_m\mathbf{x} = \sum_{i=1}^{N_{IR}}\tilde{\mathbf{h}}_m\mathbf{w}_i s_i^I + \sum_{k=1}^{N_{ER}}\tilde{\mathbf{h}}_m\mathbf{v}_k s_k^E + n, \tag{7}$$

where N_{IR} and N_{ER} are the numbers of IRs and ERs. The beamforming vectors of the energy and the information are $\mathbf{w}_i$ and $\mathbf{v}_k$. Moreover, the signals satisfy $\mathbb{E}\left\{|s|^2\right\} = 1$ and additive white Gaussian noise (AWGN) $n \sim \mathcal{CN}\left(0, \sigma^2\right)$.

Based on the above system, we set an EE maximization problem as follows.

$$(\mathbf{P0}): \max_{\{\mathbf{w}_i, \mathbf{v}_k, \mathbf{\Xi}\}} \frac{\sum_{i=1}^{N_{IR}}\log_2\left(1 + \frac{\left|\tilde{\mathbf{h}}_i\mathbf{w}_i\right|^2}{\sum_{m\neq i}^{N_{IR}}\left|\tilde{\mathbf{h}}_i\mathbf{w}_m\right|^2 + \sigma^2}\right)}{\sum_{i=1}^{N_{IR}}\left\|\mathbf{w}_i\right\|_2^2 + \sum_{k=1}^{N_{ER}}\left\|\mathbf{v}_k\right\|_2^2 + P_c + N_i P_i} \tag{8a}$$

$$\text{s.t. } \log_2\left(1 + \frac{\left|\tilde{\mathbf{h}}_i\mathbf{w}_i\right|^2}{\sum_{m\neq i}^{N_{IR}}\left|\tilde{\mathbf{h}}_i\mathbf{w}_m\right|^2 + \sigma^2}\right) \geq R_i^{(\mathrm{D})}, \forall i, \tag{8b}$$

$$\sum_{i=1}^{N_{IR}}\left\|\mathbf{w}_i\right\|_2^2 + \sum_{k=1}^{N_{ER}}\left\|\mathbf{v}_k\right\|_2^2 \leq P_{\mathrm{Max}}, \tag{8c}$$

$$\tilde{\mathbf{h}}_k\left(\sum_{i=1}^{N_{IR}}\mathbf{w}_i\mathbf{w}_i^H + \sum_{k=1}^{N_{ER}}\mathbf{v}_k\mathbf{v}_k^H\right)\tilde{\mathbf{h}}_k^H \geq \mathcal{M}(E_k^{(\mathrm{D})}), \forall k, \tag{8d}$$

$$\mathrm{Re}\left(\mathbf{\Xi}(l,l)\right) = R_0 \geq 0, \forall l, \tag{8e}$$

$$\mathrm{Im}\left(\mathbf{\Xi}(l,l)\right) \in \mathbb{R}, \forall l. \tag{8f}$$

where (8a) is the fractional form of the EE. In detail, the numerator of it is the sum rate $\sum_{i=1}^{N_{IR}} R_i\left(\mathbf{w}_i, \mathbf{\Xi}\right)$ and we assume that the IRs can eliminate the interface of the ERs. The denominator denotes the total energy consumption $P\left(\mathbf{w}_i, \mathbf{v}_k\right)$, in which P_c and P_i are the power consumption of the front-end devices and the control circuits. (8b) is the minimum rate requirement of the IRs. (8c) is the total transmitting power budget. As for the energy harvesting demand of the ERs, $E_k^{(\mathrm{D})}$ is the minimum direct-current (DC) output power demand and the corresponding $\mathcal{M}(E_k^{(\mathrm{D})}) = \upsilon - \frac{\ln(\frac{Q(1+\exp(\kappa\upsilon))}{E_k^{(\mathrm{D})}\exp(\kappa\upsilon)+Q} - 1)}{\kappa}$ is the minimum radio-frequency (RF) power need based on the non-linear rectifying model [8]. (8e) and (8f) are the control circuit constraints. Specifically, we set that the reactances can be adjusted further while the resistances are fixed. These settings can be achieved by the control circuits based on varactors, as their reactances can be configurated by the input DC voltages while keeping the resistances nearly unchanged.

III. Joint Beamforming and Hardware Parameter Optimization

A. Problem Transformation

In this work, we assume the mutual-coupling effects between the RIS elements can be ignored and thus the inverse of $\mathbf{Z}_{ii}+\mathbf{\Xi}$ in (1) can be simplified. Moreover, the total transfer model can be transformed as

$$\tilde{\mathbf{h}} = \mathbf{d} + \mathbf{c}\mathbf{\Sigma}\mathbf{K} + \mathbf{h}_c. \tag{9}$$

The above equation has a cascade form, which is easier for solving. In particular, $\mathbf{\Sigma}$ can be written as $\mathbf{\Sigma} = \operatorname{diag}\left(\frac{1}{\mathbf{Z}_{ii}(1,1)+\mathbf{\Xi}(1,1)}, \cdots, \frac{1}{\mathbf{Z}_{ii}(N_i,N_i)+\mathbf{\Xi}(N_i,N_i)}\right)$. Consistent with (8e) and (8f), we make the real part of $\mathbf{\Xi}$ fixed and the imaginary part is continuously adjustable. Further, we can introduce $a_l + jb_l$ to replace the $\mathbf{Z}_{ii}(l,l) + \mathbf{\Xi}(l,l)$, where a_l and b_l can be denoted

$$a_l = \operatorname{Re}\left(\mathbf{Z}_{ii}(l,l)\right) + R_0, \tag{10}$$

$$b_l = \operatorname{Im}\left(\mathbf{Z}_{ii}(l,l) + \mathbf{\Xi}(l,l)\right). \tag{11}$$

With them, each entities of $\mathbf{\Sigma}$ can be replaced as $\frac{1+\exp(j\Phi_l)}{2a_l}$, where $\Phi_l = 2\theta_l$ and $\tan\theta_l = -\frac{a_l}{b_l}$. Typically, $\operatorname{Re}\left(\mathbf{Z}_{ii}(l,l)\right) > 0$, thus $\Phi_l \in (0, 2\pi)$. Relying on these, we can reformulate equation (9) as

$$\tilde{\mathbf{h}} = \hat{\mathbf{d}} + \mathbf{c}\mathbf{\Theta}\mathbf{K}. \tag{12}$$

where the introduced notations are $\hat{\mathbf{d}} = \mathbf{d} + \mathbf{h}_c + \frac{\mathbf{c}\mathbf{K}}{2a_l}$ and $\mathbf{\Theta} = \operatorname{diag}(\frac{\exp(j\Phi_l)}{2a_l}, \ldots, \frac{\exp\left(j\Phi_{N_i}\right)}{2a_{N_i}})$.

Hereto, problem $(\mathbf{P}0)$ can be transformed into an equivalent form.

$$\begin{aligned}(\mathbf{P}1): &\max_{\{\mathbf{w}_i,\mathbf{v}_k,\mathbf{\Theta}\}} \mathrm{EE}(\mathbf{w}_i,\mathbf{v}_k,\mathbf{\Theta})\\ &\text{s.t. (8b)-(8d)},\\ &\quad \Phi_l \in (0,2\pi), \forall l.\end{aligned} \tag{13}$$

It can be found that although the no-mutual-coupling assumption is introduced, the above problem still is a non-convex problem with coupled variables and fractional optimization objective. For tackling it, the problem can be iteratively solved by SDR, Dinkelbach's algorithm and SCA. The total optimization framework can be found in Algorithm 1.

B. SDR approach

We apply SDR to the beamforming vectors as $\mathbf{W}_i = \mathbf{w}_i\mathbf{w}_i^H$, $\mathbf{V}_k = \mathbf{v}_k\mathbf{v}_k^H$. In addition, The constraints of the transformations are $\mathbf{W}_i \succeq 0$, $\operatorname{rank}(\mathbf{W}_i) = 1$, $\mathbf{V}_k \succeq 0$ and $\operatorname{rank}(\mathbf{V}_k) = 1$. Similarly, for the circuit parameter Φ, we utilize $\mathbf{K}_u = \operatorname{diag}(\mathbf{c})\mathbf{K}$ and $\mathbf{g} = [\frac{\exp(j\Phi_l)}{2a_l}, \ldots, \frac{\exp\left(j\Phi_{N_i}\right)}{2a_{N_i}}]$ to replace the transfer model as

$$\tilde{\mathbf{h}} = \hat{\mathbf{d}} + \mathbf{g}\mathbf{K}_u. \tag{14}$$

With $\hat{\mathbf{g}} = [\mathbf{g}, 1]$ and $\hat{\mathbf{K}}_u = [\mathbf{K}_u; \hat{\mathbf{d}}]$, equation (14) can have more concise form. And SDR also can be used to form $\hat{\mathbf{g}}$ as $\hat{\mathbf{G}} = \hat{\mathbf{g}}^H\hat{\mathbf{g}}$ subject to $\operatorname{rank}(\hat{\mathbf{G}}) = 1$ and $\hat{\mathbf{G}} \succeq 0$. When removing the rank constraints, we can present the problem as

Algorithm 1 Total alternative optimization framework

Initialize: ϵ, $\hat{\mathbf{G}}^{(0)}$
1: Set $j = 1$, $\mathcal{D}$, $\mathrm{EE}^{(0)} = 0$;
2: **while** $\mathcal{D} \le \epsilon$ **do**
3: **Repeat**
4: Use Dinkelbach's algorithm in Algorithm 2 and SCA in Algorithm 3 to resolve subproblem $(\mathbf{P}2.1)$;
5: **Until** Termination condition is met;
6: Return solved $\{\mathbf{w}_i^*, \mathbf{v}_k^*\}$;
7: **Repeat**
8: Adopt SCA in similar framework of Algorithm 3 to solve subproblem $(\mathbf{P}2.3)$;
9: **Until** Termination condition is met;
10: Return solved $\mathbf{g}^*$;
11: Calculate $\mathrm{EE}^{(j)}$ with optimized variables and reset the parameters of subproblems;
12: Set $\mathcal{D} = \mathrm{EE}^{(j)} - \mathrm{EE}^{(j-1)}$;
13: Update $j = j + 1$;
14: **end while**
Output: the optimal $\{\mathbf{w}_i^*, \mathbf{v}_k^*, \mathbf{g}^*\}$

$$(\mathbf{P}2): \max_{\{\mathbf{W}_i,\mathbf{V}_k,\hat{\mathbf{G}}\}} \frac{\sum_{i=1}^{N_{IR}} R_i\left(\mathbf{W}_i, \hat{\mathbf{G}}\right)}{P\left(\mathbf{W}_i, \mathbf{V}_k\right)} \tag{15a}$$

$$\text{s.t. } \frac{\operatorname{Tr}\left(\hat{\mathbf{G}}\hat{\mathbf{K}}_{u,i}\mathbf{W}_i\hat{\mathbf{K}}_{u,i}^H\right)}{\operatorname{Tr}\left(\hat{\mathbf{G}}\hat{\mathbf{K}}_{u,i}\sum_{m\neq i}^{N_{IR}}\mathbf{W}_m\hat{\mathbf{K}}_{u,i}^H\right) + \sigma^2} \ge 2^{R_i^{(\mathrm{D})}} - 1, \forall i, \tag{15b}$$

$$\sum_{i=1}^{N_{IR}} \operatorname{Tr}\left(\mathbf{W}_i\right) + \sum_{k=1}^{N_{ER}} \operatorname{Tr}(\mathbf{V}_k) \le P_{\mathrm{Max}}, \tag{15c}$$

$$\operatorname{Tr}\left(\hat{\mathbf{G}}\hat{\mathbf{K}}_{u,k}(\sum_{i=1}^{N_{IR}}\mathbf{W}_i + \sum_{k=1}^{N_{ER}}\mathbf{V}_k)\hat{\mathbf{K}}_{u,k}^H\right) \ge \mathcal{M}(E_k^{(\mathrm{D})}), \forall k, \tag{15d}$$

$$\hat{\mathbf{G}}(l,l) = \frac{1}{4a_l^2}, \forall l, \hat{\mathbf{G}}(N_i+1, N_i+1) = 1, \tag{15e}$$

$$\mathbf{W}_i \succeq \mathbf{0}, \mathbf{V}_k \succeq \mathbf{0}, \hat{\mathbf{G}} \succeq \mathbf{0}, \forall i, k. \tag{15f}$$

The constraint (15e) can be considered a type of hardware loss of the RIS. It is different from the common assumption that the magnitudes of reflection coefficients equal one in the IDS model, which is an ideal case of total reflection without loss.

C. Optimization framework

For tackling problem $(\mathbf{P}2)$ further, we adopt the alternative optimization strategy. First, the beamforming vectors are optimized with fixed $\hat{\mathbf{G}}$. Nevertheless, the fractional objective is still intractable. Dinkelbach's algorithm presented in Algo-

Algorithm 2 Dinkelbach's algorithm

Initialize: $\varsigma^{(0)}=0$, ϵ;

1: Set $t=0$;
2: **Repeat**
3: Resolve the problem $(\mathbf{P}2.2)$ through SCA approach in Algorithm 3 for achieving $\mathbf{W}_i^{*(t)}, \mathbf{V}_k^{*(t)}$;
4: Let

$$\mathcal{Q}^{*(t)}=\sum_{i=1}^{N_{IR}} R_i\left(\mathbf{W}_i^{*(t)}\right)-\varsigma^{(t)} P\left(\mathbf{W}_i^{*(t)}, \mathbf{V}_k^{*(t)}\right);$$

5: Update $\varsigma^{(t+1)}=\frac{\sum_{i=1}^{N_{IR}} R_i\left(\mathbf{W}_i^{*(t)}\right)}{P\left(\mathbf{W}_i^{*(t)}, \mathbf{V}_k^{*(t)}\right)}$;
6: $t=t+1$;
7: **Until** $\mathcal{Q}^{*(t)} \leq \epsilon$
8: Recover $\mathbf{w}_i^*$ and $\mathbf{v}_k^*$ by the eigenvalue decomposition, when their ranks equal one. Otherwise, Gaussian randomization is utilized [16];

Output: the optimal $\mathbf{w}_j^*$ and $\mathbf{v}_l^*$.

rithm 2 is applied to resolve it and the transformed problem can be written as

$$(\mathbf{P}2.1): \max_{\{\mathbf{W}_i, \mathbf{V}_k\}} \sum_{i=1}^{N_{IR}} R_i\left(\mathbf{W}_i\right)-\varsigma P\left(\mathbf{W}_i, \mathbf{V}_k\right) \tag{16}$$
$$\text{s.t. (15b)-(15d), (15f).}$$

Relevant proofs can be found in [17]. It needs to be mentioned that problem $(\mathbf{P}2.1)$ is just an iteration of Dinkelbach's algorithm and we omit the iteration symbols. To further solve the above problem, we introduce several variables as

$$\zeta_i=R_i\left(\mathbf{W}_i\right), \tag{17}$$

$$e^{x_i}=\operatorname{Tr}\left(\hat{\mathbf{G}} \hat{\mathbf{K}}_{u,i} \sum_{m \neq i}^{N_{IR}} \mathbf{W}_m \hat{\mathbf{K}}_{u,i}^H\right), \tag{18}$$

$$e^{y_i}=2^{\zeta_i}-1. \tag{19}$$

Based on (17)-(19), problem $(\mathbf{P}2.1)$ can be replaced by $(\mathbf{P}2.2)$.

$$(\mathbf{P}2.2): \max_{\left\{\begin{array}{c}\mathbf{w}_i, \mathbf{v}_k, \zeta_i, \\ x_i, y_i\end{array}\right\}} \sum_{i=1}^{N_{IR}} \zeta_i-\varsigma P\left(\mathbf{W}_i, \mathbf{V}_k\right)$$
$$\text{s.t.} \operatorname{Tr}\left(\hat{\mathbf{G}} \hat{\mathbf{K}}_{u,i} \mathbf{W}_i \hat{\mathbf{K}}_{u,i}^H\right) \geq e^{x_i+y_i}+\sigma^2 e^{y_i}, \forall i, \tag{20a}$$

$$e^{x_i} \geq \operatorname{Tr}\left(\hat{\mathbf{G}} \hat{\mathbf{K}}_{u,i} \sum_{m \neq i}^{N_{IR}} \mathbf{W}_m \hat{\mathbf{K}}_{u,i}^H\right), \forall i, \tag{20b}$$

$$e^{y_i} \geq 2^{\zeta_i}-1, \forall i, \tag{20c}$$
$$\text{(15b)-(15d), (15f).}$$

Applying first-order approximation to the left hands of (20b) and (20c), we can get

$$e^{x_i} \geq e^{\bar{x}_i}+e^{\bar{x}_i}\left(x_i-\bar{x}_i\right), \tag{21}$$

$$e^{y_i} \geq e^{\bar{y}_i}+e^{\bar{y}_i}\left(y_i-\bar{y}_i\right), \tag{22}$$

Algorithm 3 SCA method

Initialize: $\bar{x}_i^{(0)}$, $\bar{y}_i^{(0)}$, ϵ;

1: Set $n=1$;
2: **Repeat**
3: Solve $(\mathbf{P}2.2)$ to achieve optimized beamforming vectors;
4: Update $\zeta_i^{*(n)}$, $\bar{x}_i^{*(n)}$ and $\bar{y}_i^{*(n)}$
5: $n=n+1$;
6: **Until**
7: $\left|\bar{x}_i^{*(n)}-\bar{x}_i^{*(n-1)}\right| \leq \epsilon$ and $\left|\bar{y}_i^{*(n)}-\bar{y}_i^{*(n-1)}\right| \leq \epsilon$

Output: the optimal $\mathbf{W}_j^{*(n)}$ and $\mathbf{V}_l^{*(n)}$

where $\bar{x}_i$ and $\bar{y}_i$ are feasible points of the problem. When substituting (20b) and (20c) of problem $(\mathbf{P}2.2)$ by thier right hands, we can get the following equations.

$$e^{\bar{x}_i}+e^{\bar{x}_i}\left(x_i-\bar{x}_i\right) \geq \operatorname{Tr}\left(\hat{\mathbf{G}} \hat{\mathbf{K}}_{u,i} \sum_{m \neq i}^{N_{IR}} \mathbf{W}_m \hat{\mathbf{K}}_{u,i}^H\right), \tag{23a}$$

$$e^{\bar{y}_i}+e^{\bar{y}_i}\left(y_i-\bar{y}_i\right) \geq 2^{\zeta_i}-1. \tag{23b}$$

Then the problem turns into a solvable convex problem, which can be tackled by the CVX program. Nevertheless, for ensuring accuracy, the problem should be resolved iteratively through the SCA approach in Algorithm 3. In each SCA iteration, problem $(\mathbf{P}2.2)$ is solved and then transfers the optimized parameters into the next solution until the termination condition is met. The variables in it can be updated as following equations.

$$\zeta_i^*=\log_2\left(1+\frac{\operatorname{Tr}\left(\hat{\mathbf{G}} \hat{\mathbf{K}}_{u,i} \mathbf{W}_i^* \hat{\mathbf{K}}_{u,i}^H\right)}{\operatorname{Tr}\left(\hat{\mathbf{G}} \hat{\mathbf{K}}_{u,i} \sum_{m \neq i}^{N_{IR}} \mathbf{W}_m^* \hat{\mathbf{K}}_{u,i}^H\right)+\sigma^2}\right), \tag{24}$$

$$\bar{x}_i^*=\ln\left(\operatorname{Tr}\left(\hat{\mathbf{G}} \hat{\mathbf{K}}_{u,i} \sum_{m \neq i}^{N_{IR}} \mathbf{W}_m^* \hat{\mathbf{K}}_{u,i}^H\right)\right), \tag{25}$$

$$\bar{y}_i^*=\ln(2^{\zeta_i^*}-1). \tag{26}$$

With given $\mathbf{W}_i^*$ and $\mathbf{V}_k^*$, problem $(\mathbf{P}2)$ can also utilize the same transformations and approximations for optimizing $\hat{\mathbf{G}}$.

$$(\mathbf{P}2.3): \max_{\{\hat{\mathbf{G}}, \varpi_i, c_i, d_i\}} \sum_{i=1}^{N_{IR}} \varpi_i$$
$$\text{s.t.} \operatorname{Tr}\left(\hat{\mathbf{G}} \hat{\mathbf{K}}_{u,i} \mathbf{W}_i \hat{\mathbf{K}}_{u,i}^H\right) \geq e^{c_i+d_i}+\sigma^2 e^{d_i}, \forall i, \tag{27a}$$

$$e^{\bar{c}_i}+e^{\bar{c}_i}\left(c_i-\bar{c}_i\right) \geq \operatorname{Tr}\left(\hat{\mathbf{G}} \hat{\mathbf{K}}_{u,i} \sum_{m \neq i}^{N_{IR}} \mathbf{W}_m \hat{\mathbf{K}}_{u,i}^H\right), \forall i, \tag{27b}$$

$$e^{\bar{d}_i}+e^{\bar{d}_i}\left(d_i-\bar{d}_i\right) \geq 2^{\varpi_i}-1, \forall i, \tag{27c}$$
$$\text{(15b),(15d)-(15f).}$$

The SCA method still can operate in problem $(\mathbf{P}2.3)$. Then for recovering the original vector $\mathbf{g}$, the Gaussian randomization and eigenvalue decomposition approaches are allied

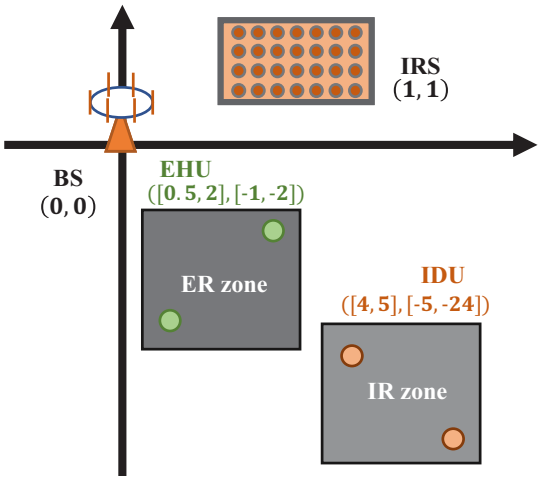

Fig. 1: The experiment setting.

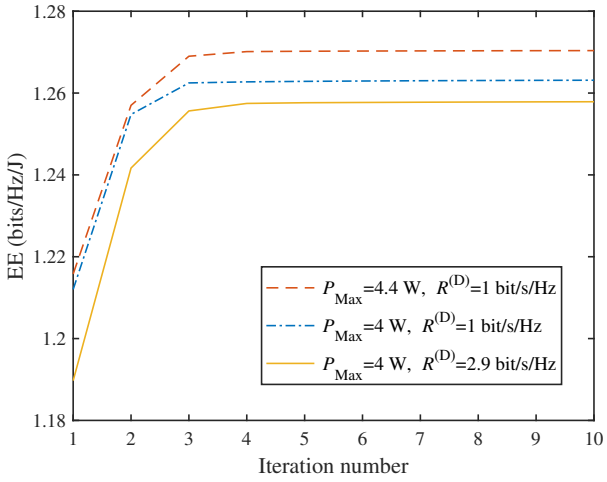

Fig. 2: Convergence behaviors of the proposed scheme.

according to the different conditions and the details can be found in [16]. Through the alternative optimization strategy, the beamforming vectors and $\hat{\mathbf{G}}$ can be solved iteratively until the final ending condition is achieved as in Algorithm 1.

IV. Numerical Results

The BS, a linear array with 8 elements, and the RIS, a 2×8 rectangular array, are located at (0,0) and (1,1), respectively. Moreover, two IRs and two ERs appear in the zone ([4,5],[-5,-24]) and the zone ([0.5,2],[-1,-2]). The antennas have half-wavelength lengths and operate at 28GHz. the element spacings of the BS and the RIS are half wavelength and quarter wavelength. The cluster number and path number of scatterer links follow $N_{\text{sca}} \sim \max\{\text{Poisson}(1.8), 1\}$ and $N_{\text{path}} \sim U(0, 30)$ [15]. Additionally, Complex gain and angles of departure follow $\beta_{p,q} \sim \mathcal{CN}(0, 1)$ and Laplacian distribution. The remaining default settings are $E^{(\text{D})} = 1.3\mu$W, $R^{(\text{D})} = 1$bit/s/Hz, $P_c = 1$ W, $P_I = 10$ mW, $\sigma^2 = 1 \times 10^{(-12)}$W and $P_{\text{Max}} = 4$W. The circuit parameters of

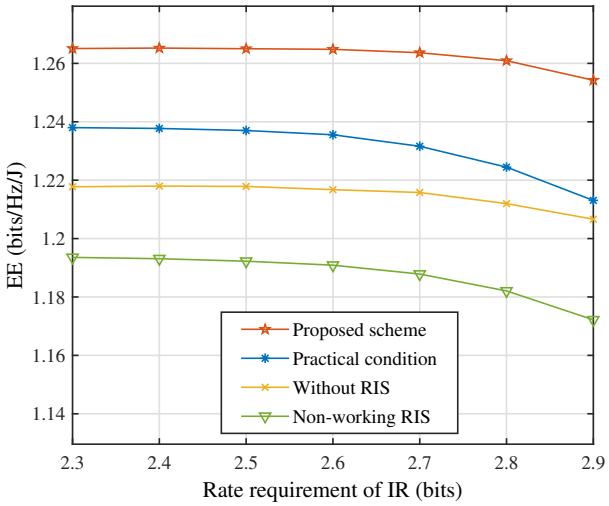

Fig. 3: EE versus rate requirements of IR.

the nonlinear recovering model are $Q = 9.804$, $\upsilon = -1.293$ and $\kappa = 0.119$.

The convergence behaviors of the total optimization framework are shown in Fig. 2 and the effectiveness of the scheme is presented. It can be found that about three iterations of the proposed framework are able to make the EE performance stable under the different experiment settings.

In Fig. 3, the trends of all various conditions are similar, which is declining as the improving rate requirements of IRs. The reason for this phenomenon is that the IRs with better channel conditions may be allocated more resources when the rate requirements are slack for achieving a greater sum rate. However, as the rate needs of all IRs increase simultaneously, the power resource should be distributed more to the worse-channel-condition IRs, which makes it harder to consider the total EE level. In addition, the proposed scheme has a better performance compared to the no-RIS and non-working-RIS cases, which indicates that the RIS can improve EE of the system. However, it is remarkable that there are performance losses between the ideal case and the practical condition, the case of considering the mutual-coupling effects.

In Fig. 4, the performance differences among all conditions keep in line with Fig. 3. Moreover, it can be found that the EE performances enhance as the transmitting power levels improve in all cases. In detail, the rates of EE improvement slow down gradually, which is because the consequently increased interference levels cause negative effects on EE. Moreover, since enhanced power input doesn't bring a large gain to the sum rate, the EE performance, the tradeoff between the rate and the energy consumption, is locked at the end of growth.

In Fig. 5, we conduct the simulation through HFSS 2021 for analyzing the practical beams. Considering clarity, we set only a pair of IR and ER, located at (10,-11) and (0.5,-2), respectively. The angles of BS-ER and BS-RIS are -14° and

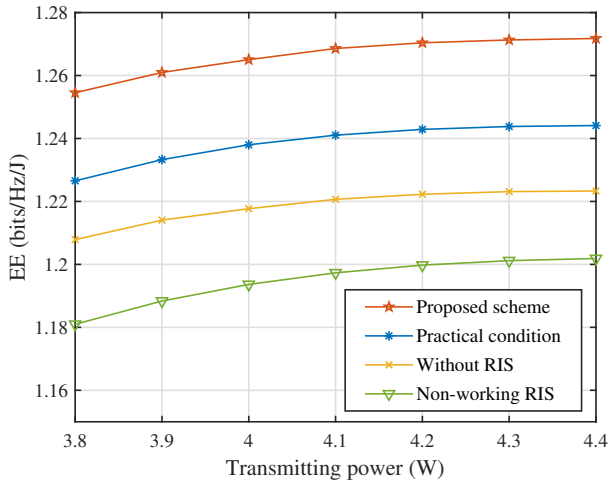

Fig. 4: EE versus power budget of BS.

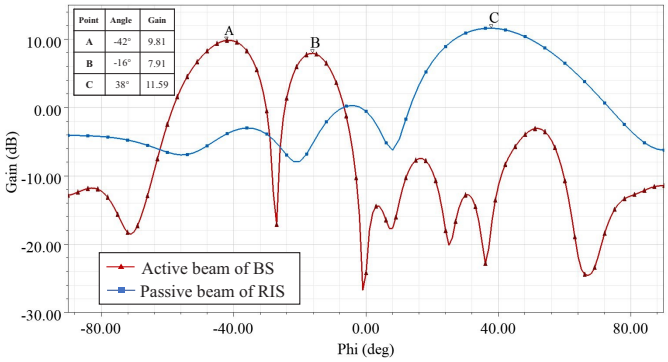

Fig. 5: Generated beams of the BS and RIS through the proposed optimization framework.

$-45°$. From Fig. 5, it can be seen that the generated two sub-beams of the BS point at $-16°$ and $-42°$ for serving the ER and acting as an incident beam of the RIS. The differences between actual angles and the directions of sub-beams are inconspicuous, which demonstrates the effectiveness of the proposed scheme. Furthermore, the passive beam points at $38°$, which also is close to the actual angle of RIS-IR, $39°$. The above results illustrate that the BS mainly satisfies the requirement of the ER and the RIS plays an indispensable role in serving the IR under this experiment setting.

V. Conclusion

In this paper, we adopted a transfer model of mixed determinate EM entities and random scatterers to present the influences of the hardware attributes on the system performances. Particularly, the optimizable variables were no longer the reflection coefficients but the impedances of the control circuits. Due to this setting, the practical variables can be adopted into the hardware design directly. The introduced EE maximization problem was transformed into a more solvable form. Further, it can be decomposed into two sub-problems and then the SDR transformation, Dinkelbach's algorithm and SCA method were utilized to resolve them, respectively. The results of the numerical experiments demonstrate the proposed optimization framework is effective. In addition, the actual beam forms of the BS and the RIS meet the expectations. As for future work, we will concentrate on more compatible RIS models and related application scenarios.

References

[1] M. Z. Chowdhury, M. Shahjalal, S. Ahmed, and Y. M. Jang, "6G wireless communication systems: Applications, requirements, technologies, challenges, and research directions," *IEEE Open Journal of the Communications Society*, vol. 1, pp. 957–975, 2020.

[2] M. Giordani, M. Polese, M. Mezzavilla, S. Rangan, and M. Zorzi, "Toward 6G networks: Use cases and technologies," *IEEE Communications Magazine*, vol. 58, no. 3, pp. 55–61, 2020.

[3] Y. Zhang, S. Han, W. Meng, X. Li, and Y. Chen, "Asymptotic analysis and precoding design of integrated access and backhaul in full-duplex mmwave networks," *China Communications*, vol. 19, no. 5, pp. 24–45, 2022.

[4] S. Han, Z. Gong, W. Meng, C. Li, D. Zhang, and W. Tang, "Automatic precision control positioning for wireless sensor network," *IEEE Sensors Journal*, vol. 16, no. 7, pp. 2140–2150, 2016.

[5] D. C. Nguyen, M. Ding, P. N. Pathirana, A. Seneviratne, J. Li, D. Niyato, O. Dobre, and H. V. Poor, "6G internet of things: A comprehensive survey," *IEEE Internet of Things Journal*, vol. 9, no. 1, pp. 359–383, 2022.

[6] A. Costanzo, D. Masotti, G. Paolini, and D. Schreurs, "Evolution of SWIPT for the IoT world: Near- and far-field solutions for simultaneous wireless information and power transfer," *IEEE Microwave Magazine*, vol. 22, no. 12, pp. 48–59, 2021.

[7] Q. Wu and R. Zhang, "Towards smart and reconfigurable environment: Intelligent reflecting surface aided wireless network," *IEEE Communications Magazine*, vol. 58, no. 1, pp. 106–112, 2019.

[8] S. Zargari, A. Khalili, Q. Wu, M. Robat Mili, and D. W. K. Ng, "Max-min fair energy-efficient beamforming design for intelligent reflecting surface-aided SWIPT systems with non-linear energy harvesting model," *IEEE Transactions on Vehicular Technology*, vol. 70, no. 6, pp. 5848–5864, 2021.

[9] C. L. Holloway, E. F. Kuester, J. A. Gordon, J. O'Hara, J. Booth, and D. R. Smith, "An overview of the theory and applications of metasurfaces: The two-dimensional equivalents of metamaterials," *IEEE Antennas and Propagation Magazine*, vol. 54, no. 2, pp. 10–35, 2012.

[10] X. Yu, V. Jamali, D. Xu, D. W. K. Ng, and R. Schober, "Smart and reconfigurable wireless communications: From IRS modeling to algorithm design," *IEEE Wireless Communications*, vol. 28, no. 6, pp. 118–125, 2021.

[11] M. Najafi, V. Jamali, R. Schober, and H. V. Poor, "Physics-based modeling and scalable optimization of large intelligent reflecting surfaces," *IEEE Transactions on Communications*, vol. 69, no. 4, pp. 2673–2691, 2021.

[12] S. Abeywickrama, R. Zhang, Q. Wu, and C. Yuen, "Intelligent reflecting surface: Practical phase shift model and beamforming optimization," *IEEE Transactions on Communications*, vol. 68, no. 9, pp. 5849–5863, 2020.

[13] G. Gradoni and M. Di Renzo, "End-to-end mutual coupling aware communication model for reconfigurable intelligent surfaces: An electromagnetic-compliant approach based on mutual impedances," *IEEE Wireless Communications Letters*, vol. 10, no. 5, pp. 938–942, 2021.

[14] Q. Wu and R. Zhang, "Weighted sum power maximization for intelligent reflecting surface aided SWIPT," *IEEE Wireless Communications Letters*, vol. 9, no. 5, pp. 586–590, 2020.

[15] M. R. Akdeniz, Y. Liu, M. K. Samimi, S. Sun, S. Rangan, T. S. Rappaport, and E. Erkip, "Millimeter wave channel modeling and cellular capacity evaluation," *IEEE journal on selected areas in communications*, vol. 32, no. 6, pp. 1164–1179, 2014.

[16] Z.-q. Luo, W.-k. Ma, A. M.-c. So, Y. Ye, and S. Zhang, "Semidefinite relaxation of quadratic optimization problems," *IEEE Signal Processing Magazine*, vol. 27, no. 3, pp. 20–34, 2010.

[17] W. Dinkelbach, "On nonlinear fractional programming," *Management science*, vol. 13, no. 7, pp. 492–498, 1967.